

An attempt to find precursors in the ULF geomagnetic data by means of flicker noise spectroscopy

M. Hayakawa¹ and S. F. Timashev²

¹Department of Electronic Engineering, The University of Electro-Communications, Chofu Tokyo 182-8585, Japan

²Karpov Institute of Physical Chemistry, Moscow 103064, Russia

Received: 23 January 2006 – Revised: 20 March 2006 – Accepted: 20 March 2006 – Published: 3 July 2006

Abstract. The flicker noise spectroscopy which is a new phenomenological method for the retrieval of information contained in chaotic time signals, is based on the analysis of recognizable irregularities (pulse, jumps, and discontinuities of derivatives of various order). This method is applied to the ULF (ultra-low-frequency) data observed at Guam in 1992–1994, in order to study the temporal nonlinear behavior of the lithospheric activity prior to the large 1993 Guam earthquake (8 August 1993). We have found that the lithosphere must have exhibited the step-like discontinuous behaviors in the lithosphere 101, 78, 54, 31 and 8 days before the main shock. This kind of nonlinear temporal behavior can be tracked by means of our flicker noise spectroscopy.

1 Introduction

We understand that when a heterogeneous material is strained, its evolution toward the final rupture is characterized by the nucleation and coalescence of microcracks before the final rupture. The two physical quantities are recognized as being most indicative of microfracturing process in the focal zone; (1) ULF electromagnetic emissions and (2) acoustic emissions (Hayakawa, 2001, 2004; Hayakawa et al., 2004). Though there have recently been found a lot of convincing evidence on the electromagnetic emissions in a wide frequency range from DC, ULF to VHF associated with earthquakes (e.g. Hayakawa and Fujinawa, 1994; Hayakawa, 1999; Hayakawa and Molchanov, 2002), but our main tool in this paper is to monitor such microfractures which are known to occur before the final breakup in the focal zone of an earthquake, by recording the ULF emissions. The presence of precursory signature of earthquakes is clearly identified in the ULF range for large (magnitude greater than 7) earthquakes

such as Spitak, Loma Prieta, Guam, Biak etc. (Fraser-Smith et al., 1990; Molchanov et al., 1992; Kopytenko et al., 1993; Hayakawa et al., 1996, 1999, 2000).

The ULF emissions are found to take place from a few weeks to a few days prior to large destructive earthquakes (including Spitak, Loma Prieta, Guam etc.), which are considered as the so-called precursors of the general fracture. The emissions in higher frequency range (like VLF and HF/VHF) (Kapiris et al., 2004) are likely to be occurring in the focal zone of an earthquake, but they cannot be detected on the Earth's surface because of their extremely severe attenuation in the crust. So, those higher frequency emissions might be generated as secondary effect near the Earth's surface, and their generation mechanism is poorly understood at the moment. In comparison with this, the ULF emissions are believed to be definitely generated in the focal zone and to have propagated up to the subsurface ULF sensors. Dynamic process in seismo-active areas can produce current systems of different kind (see e.g. Molchanov and Hayakawa, 1995; Vallianatos and Tzanis, 1999, and references therein), which can be local source for electromagnetic waves at different frequencies. The ULF range is the most possible to come from the source region with the least attenuation. Based on these arguments, we can consider that those ULF emissions would carry the information on the microfracturing taking place near the focal zone. Molchanov and Hayakawa (1995) proposed the generation mechanism of seismogenic ULF emissions on the basis of microfracturing.

Because the dynamics of earthquakes is well known to exhibit properties which are characteristics for the self-organized criticality (SOC) state (e.g. Bak et al., 1987; Bak, 1997), we have made the first attempt to use the fractal analysis to the seismogenic ULF emissions as a nonlinear process for the Guam earthquake (Hayakawa et al., 1999). Because the principal feature of the SOC state is a fractal organization of the output parameters both in space (scale-invariant structure) and in time (flicker noise or $1/f$ noise). If the time series

Correspondence to: M. Hayakawa
(hayakawa@whistler.ee.uec.ac.jp)

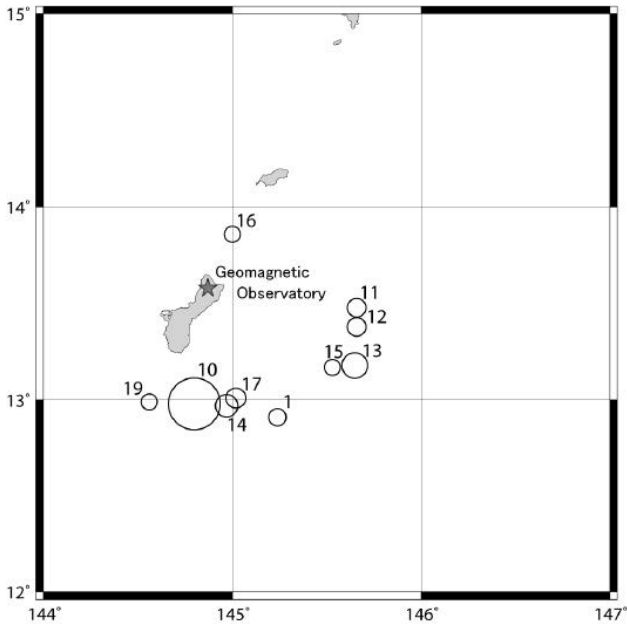


Fig. 1. Location of epicenters of earthquakes taken place close to the ULF observing station. No. 10 earthquake is the one we pay particular attention in this paper, and others (Nos. 11–19) are its aftershocks. The number in this figure is corresponding to that in Table 1.

of ULF data is a temporal fractal, we expect a power-law spectral density of the recorded time series: $S(f) \propto f^{-\beta}$ (β : spectral exponent). Hayakawa et al. (1999) have found a significant change in this spectral exponent (β) just before the Guam earthquake in such a way that the value of β is approaching unity (becoming flicker noise) before the rupture, and later the similar behavior has also been confirmed for another large earthquake at Biak (Hayakawa et al., 2000). This estimation of fractal dimension was based on the spectral slope, β in the spectral analysis, but later Smirnova et al. (2001) and Gotoh et al. (2003, 2004) have compared different analysis methods in estimating the fractal dimension (spectral slope, Burlaga and Klein (1986) and Higuchi (1988) methods). The seismicity spatial and temporal distribution is known to reveal statistically self-similar properties in a wide range of scales and can be treated as multifractal (e.g. Turcotte, 1997). Our previous studies are just based on monofractal analysis, and the multi-fractal analysis for the same Guam earthquake has yielded that multi-fractal parameters would bring us a lot of precursory signatures of an earthquake (Ida et al., 2005).

In this paper we propose a new method of flicker noise spectroscopy (FNS) (Timashev, 2001; Timashev and Vstovskiy, 2003) to be used for the detection of possible precursors of catastrophic events on the basis of analysis of experimentally measured time series of dynamic variables characterizing the crustal activity of the geological medium. The

capabilities of this method make it possible to transfer the general ideas formulated by Erokhin and Moiseev (2003) to the level of general phenomenology. As distinct from all available methods of time series analysis, new understanding of the information carried by chaotic signals is introduced in the FNS approach. Irregularities of measured signals at all levels of the space-time hierarchy of the system are carriers of such information. Among the arguments favoring such a representation of the information carrier, we can mention the success of numerous computer model calculations implemented within the framework of the SOC paradigm (Bak, 1997). This method is applied to the ULF data during the 1993 Guam earthquake for which the previous studies have already confirmed the precursory signatures of the earthquake (Hayakawa, et al., 1996, 1999; Smirnova et al., 2001; Gotoh et al., 2003, 2004; Ida et al., 2005).

2 Experimental ULF data and Guam earthquake

The details of the ULF data for the Guam earthquake have already been given in Hayakawa et al. (1999), but we have to repeat only the important points as follows. The period of data analysis is from January 1992 to the end of 1994 (total three years). During this 3-years period, we could identify many earthquakes in the latitude range from 10° to 16° and in the longitude range from 140° to 147° just around the Guam ULF observatory (which is indicated as a star in Fig. 1). The total number of earthquakes with magnitude greater than 5.5 is found to be 21. Table 1 is the list of all of those earthquakes. The numbering of earthquake is given according to the time of occurrence. Figure 1 illustrates the epicenters of ten earthquakes among 21, which took place very close to the ULF station (with distance less than 100 km). As seen from the table, No. 10 is our target earthquake, and this Guam earthquake with magnitude $M_s=8.2$, occurred on 8 August 1993 at 08:34 UT suddenly and without any fore shocks. Its epicenter was located in the sea near the Guam island (geographic coordinates: 12.89 N, 144.80 E), and its depth was 60 km. The Guam observatory where the ULF data were recorded, is located at ~ 65 km from the epicenter. As seen from the table, the earthquakes with Nos. 2–9 did not take place within the distance of 100 km from the ULF observatory. This is the reason why we can say that this earthquake appeared as an extremely isolated event. We here comment on the sensitivity distance of seismogenic ULF emissions. Hayakawa and Hattori (2000) have summarized all of the previous ULF emissions, who have concluded that the distance of sensitivity of VLF emissions is approximately 100 km even for an earthquake with magnitude 7.0.

Figure 1 illustrates the relative location of our ULF observatory with respect to the epicenter. A regular magnetic observation is maintained there using a three-axis ring-core-type fluxgate magnetometer (Hayakawa et al., 1996). Three components of magnetic variations are usually recorded on

a digital cassette tape with a sampling rate of 1 s. We analyze the data during the whole period, and we analyze the data during daytime (LT=14:00–15:00), because Gotoh et al. (2004) have found that the most significant change in the mono-fractal dimension was observed for the Guam earthquake during daytime. One hour data are treated, so that the number of data is 3600 point per day.

3 Basic FNS relations for stationary processes

A new type of information contained in chaotic time series $V(t)$ (t is time), is introduced in the frame of FNS (Timashev, 2001). According to this phenomenological approach, the main information hidden in a chaotic signal at an interval T is provided by sequences of distinguishing types of irregularities – spikes, jumps, and discontinuities of derivatives of different orders at all space-time hierarchical levels of systems. In this case it is possible to introduce different types of information. The ability to distinguish the irregularities means that the parameters or patterns characterizing the totality of properties of the irregularity sequences, are extracted from the following power spectra $S(f)$ (f , frequency).

$$S(f) = \left| \int_{-T/2}^{T/2} \langle V(t)V(t+t_1) \rangle \cdot \exp(2\pi i f t_1) dt_1 \right|,$$

$$\langle \dots \rangle = \frac{1}{T} \int_{-T/2}^{T/2} (\dots) dt, \tag{1}$$

and the difference moments $\Phi^{(2)}(\tau)$ of the 2nd order,

$$\Phi^{(2)}(\tau) = \langle [V(t) - V(t+\tau)]^2 \rangle = \left\langle \left[\int_t^{t+\tau} \frac{dV(x)}{dx} dx \right]^2 \right\rangle, \tag{2}$$

where τ is time delay.

In this case, $\Phi^{(2)}(\tau)$ is formed exclusively by jumps of the dynamic variable at different space-time hierarchical levels of the system under consideration, and $S(f)$ is formed by spikes and jumps. In other words, the power spectra and difference moments of the 2nd order carry different information, which complement each other. The characteristic information extracted from the $S(f)$ and $\Phi^{(2)}(\tau)$ dependencies are the “passport parameters”, which are the correlation times, parameters characterizing the loss of “memory” for these correlation times, characterizing the sequences of “spikes”, “jumps” and discontinuities of derivatives of different orders (in the latter case, time series for “quasi-derivatives” are formed).

In the case of “stationary” processes the “passport parameters” do not depend on the position of the T interval at the time axis as well as on the frequency. The contributions $S_S(f)$ and $S_R(f)$ due only to the spike-type and jump-type

irregularities corresponding to the power spectrum $S(f)$, are presented as:

$$S_S(f) \approx \frac{S_S(0)}{1 + (2\pi f T_0)^{n_0}},$$

$$S_R(f) = \int_0^\infty \cos(2\pi f \tau) \left[\Phi^{(2)}(\infty) - \Phi^{(2)}(\tau) \right] d\tau. \tag{3}$$

Here $S_S(0)$ is an effective phenomenological parameter; n_0 is the rate of “memory (correlation) loss” in a sequence of spikes within time intervals shorter than the correlation time T_0 , $T_0^{-1} \equiv K_0$. The contribution $S_R(f)$ can be found using the expression for $\Phi^{(2)}(\tau)$.

$$\Phi^{(2)}(\tau) = 2\sigma^p \cdot \left[1 - \Gamma^{-1}(H) \cdot \Gamma(H, \tau/T_1) \right]^2,$$

$$\Gamma(s, x) = \int_x^\infty \exp(-t) \cdot t^{s-1} dt, \Gamma(s) = \Gamma(s, 0). \tag{4}$$

Here σ is the variance of the measured dynamic variable; the parameter H has the sense of the Hurst constant which characterizes the rate at which the dynamic variable “forgets” its value within time intervals shorter than T_1 ; $\Gamma(s)$ and $\Gamma(s, x)$ are the gamma and incomplete gamma functions ($x \geq 0$ and $s > 0$), respectively. The introduced parameter $S_S(0)$, n_0 , T_0 , H , T_1 and σ can be considered as “passport” parameters of the stationary process under consideration.

The term $S_R(f)$ can be expressed by the interpolation equation:

$$S_R(f) \approx S_R(0) \frac{1}{1 + (2\pi f T_1)^{2H+1}},$$

$$S_R(0) = 4\sigma^2 T_{01} H \cdot \left\{ 1 - \frac{1}{2H_\Gamma^2(H)} \int_0^\infty \Gamma^2(H, \xi) d\xi \right\}. \tag{5}$$

It is important to note that both the contributions $S_S(f)$ and $S_R(f)$ to the power spectrum $S(f)$ are similar, although the corresponding parameters in Eqs. (3) and (5) generally differ from each other: $S_R(0) \neq S_S(0)$, $T_1 \neq T_0$ and $2H \neq n_0 - 1$. It is possible to separate both contributions (3) and (5) in the “experimental” power spectra using the known parameters H and T_1 .

However, in the most real cases, $S(f)$ and $\Phi^{(2)}(\tau)$ dependencies manifest their complexity and non-stationary behavior. Then, the introduction of “passport parameters” to describe the temporal evolution is useless. At the same time, the behavior of the real $S(f)$ and $\Phi^{(2)}(\tau)$ is very specific and individual to each study case. These dependences have a definite physical sense and characterize the sequences of spikes, jumps and discontinuities of derivatives of different orders (in the latter case the time series for “quasi-derivatives” are analyzed). That is why these dependences can be considered as “characteristic passport patterns” of the evolution

Table 1. List of earthquakes in the vicinity of the Guam observatory.

Number	Date (1992–1994)	Time (UT)	Epicenter Geomagnetic		Magnitude (M>5.5)	Depth (km)
			Latitude (° N)	Longitude (° E)		
1	20 Feb 1992	17:47:20	12.91	145.24	5.6	44
2	29 Feb 1992	05:42:45	12.27	141.24	5.5	32
3	22 June 1992	15:17:43	16.87	147.01	5.7	65
4	24 Oct 1992	22:16:07	11.83	142.05	5.5	43
5	4 Feb 1993	16:28:32	12.49	141.92	5.7	27
6	5 Feb 1993	06:37:23	12.54	141.99	5.5	50
7	5 Feb 1993	07:15:21	12.57	141.88	5.9	27
8	4 June 1993	03:06:35	11.8	142.49	5.6	24
9	6 June 1993	13:23:20	15.82	146.6	6.6	13
10	8 Aug 1993	08:34:24	12.98	144.8	8.2	59
11	8 Aug 1993	20:03:14	13.48	145.66	5.7	56
12	9 Aug 1993	09:15:16	13.38	145.66	5.7	61
13	11 Aug 1993	14:17:37	13.18	145.65	6.2	21
14	16 Aug 1993	04:33:48	12.97	144.97	6	18
15	19 Aug 1993	08:03:22	13.17	145.53	5.5	60
16	4 Sep 1993	06:11:37	13.86	145	5.5	25
17	26 Sep 1993	11:55:52	13.01	145.02	5.8	63
18	7 March 1994	04:44:57	11.74	140.1	5.6	25
19	15 April 1994	19:41:07	12.99	144.56	5.5	33
20	13 Aug 1994	22:07:09	15.17	145.84	5.5	87
21	5 Nov 1994	10:52:15	10.72	141.31	5.6	31

under study. For raising the pattern specificity we split the considered signal into “low frequency” $V_R(t)$ and “high frequency” $V_F(t)$ components. The introduced decomposition $V_G(t) = V_R(t) + V_F(t)$ gives a possibility to find new characteristic features of the signals studied. The $V_R(t)$ term is obtained by using a relaxation (“diffusive” or “heat conductivity”) procedure for the total set of the initial time series readings:

$$\frac{\partial V}{\partial \tau} = \chi \frac{\partial^2 V}{\partial t^2}, \quad (6)$$

is given by that in the form of a finite difference equation

$$\frac{V_k^{j+1} - V_k^j}{\Delta \tau} = \chi \frac{V_{k+1}^j + V_{k-1}^j - 2V_k^j}{(\Delta t)^2}. \quad (7)$$

or

$$V_k^{j+1} = V_k^j + \frac{\chi \Delta \tau}{(\Delta t)^2} (V_{k+1}^j + V_{k-1}^j - 2V_k^j). \quad (8)$$

Assuming $\omega = \frac{\chi \Delta \tau}{(\Delta t)^2}$, the latter equation can be rewritten as

$$V_k^{j+1} = \omega V_{k+1}^j + \omega V_{k-1}^j + (1 - 2\omega) V_k^j, \quad (9)$$

which is absolutely stable for $\omega < 1/2$. The boundary conditions of Eq. (7) ($k=1$ and $k=N$, where N is the length of the time series) are calculated by

$$\begin{aligned} V_1^{j+1} &= (1 - 2\omega) V_1^j + 2\omega V_2^j, \\ V_M^{j+1} &= (1 - 2\omega) V_M^j + 2\omega V_{M-1}^j. \end{aligned} \quad (10)$$

Therefore, by calculating iteratively V_k^{j+1} from V_k^j , we obtain the low frequency component V_R . The high frequency component V_F is simply obtained by subtracting V_R from the original signal. We can calculate $S(f)$ and $\Phi^{(2)}(\tau)$ for each of the functions $V_J(t)$ ($J=R, F$ or G), where the subscripts R, F and G refer to $V_R(t), V_F(t)$ and $V(t)$, respectively. In these cases the corresponding subscripts for $S(f)$ and $\Phi^{(2)}(\tau)$ will be used.

4 Analysis of non-stationary processes

While studying non-stationary processes, dynamics of the $S(f)$ and $\Phi^{(2)}(\tau)$ variations is being analyzed at sequential shift of the averaging interval $[k\Delta T, t_k]$ with the extension T , where $k=0,1,2,3,\dots$ and $t_k=T+k\Delta T$, for the value ΔT along the whole time interval T_{tot} ($T+\Delta T < T_{\text{tot}}$) of the available experimental data. The time intervals T and ΔT should be selected as based on the physical sense of the considered problem – revealing the typical time of a process which determines the most important internal structural reconstruction of the studied evolution. So, if some “secondary” processes with typical times τ_i slightly affecting the main non-stationary process of the structure reconstruction occur, the condition $\tau_i \ll T$ should be observed when selecting an interval T . It is obvious that a problem of identification of typical time of the “main” process is oriented at a solution of a problem of prediction of the complex system evolution

and first and foremost – at determination of “precursors” of catastrophic changes in the system. In the conditions of “non-stationary” evolution, a system is characterized by a set of typical times T_{sr} “structural reconstructions” for a corresponding set of scales of the system’s spatial organization, and a problem of prognosis in a general case becomes multi-parametrical being oriented at a search, at least, for several time “precursors” of a catastrophic event scattered by the time scale. Each of these “precursors” can be revealed by the analysis of the dynamic variables’ time series with a selection of a certain interval of averaging T , which does not exceed the value T_{sr} being identified.

It is obviously natural to associate a phenomenon of “precursor” occurrence with the sharper variations of the relations $S(f)$ and $\Phi^{(2)}(\tau)$ at the approach of the upper boundary of the time interval of averaging t_k to a moment t_c of a catastrophic event when reconstruction takes place at all the possible spatial scales in the system. It is also natural to expect (in this case we may speak about a “precursor”) that the time of the “precursor’s” manifestation t_k should stand from the moment t_c not less than at an interval ΔT , i.e. $\Delta T_{cn} = t_c - t_k \geq \Delta T$, at realization of the inequality $\Delta T_{cn} \ll T_{tot}$. When revealing a “precursor”, it is important to distinguish cases when sharp variations in $S(f)$ and $\Phi^{(2)}(\tau)$ at averaging interval T shift are caused by significant signal variations on the “front” or “back” boundary of the interval T by approaching the “front” boundary t_k to a moment t_c of the expected event. A given problem is being solved by the analysis of the time behavior of the corresponding criteria at the T variations: it is obvious that when T increases in a value ΔT_1 the non-stationary effects associated with the signal behavior at the “back” boundary should be displayed with the same time delay ΔT_1 , when the factor display caused by sharp signal variations in the area of the front boundary does not depend so strong on the averaged interval value. Next we consider the “precursors” that are defined by the difference moments $\Phi^{(2)}(\tau)$. These functions can be reliably calculated only for a delay τ in the range $[0, \alpha T]$ with $\alpha \leq 0.5$. Let us introduce the dimensionless quantities:

$$C(t_{k+1}) = 2 \cdot \frac{Q_{k+1} - Q_k}{Q_{k+1} + Q_k} \frac{\Delta T}{T};$$

$$Q_k = \int_0^{\alpha T} [\Phi^{(2)}(\tau)]_k d\tau. \quad (11)$$

Here $t_{k+1} = k\Delta T$ ($k=0, 1, 2, \dots$) and subscripts of square brackets show that $\Phi^{(2)}(\tau)$ dependence was calculated for time interval $[k\Delta T, k\Delta T + T]$. The introduced quantities characterize a measure or factor of non-stationarity of the signals, as the averaging interval T moves along time axis by a step ΔT , in particular, when the “forward” boundary of the averaging interval t_k approaches the catastrophic event at time t_c . Evidently $C(t_{k+1}) = 0$ for the stationary processes

at $T \rightarrow \infty$. Note the $\Phi^{(2)}(\tau)$ dependence may be calculated with using the functions $V_J(t)$ ($J=R, F$).

5 Analysis results for the guam data by using FNS (z-component)

We have used the ULF data during three years from 1 January 1992 to the end of 1994.

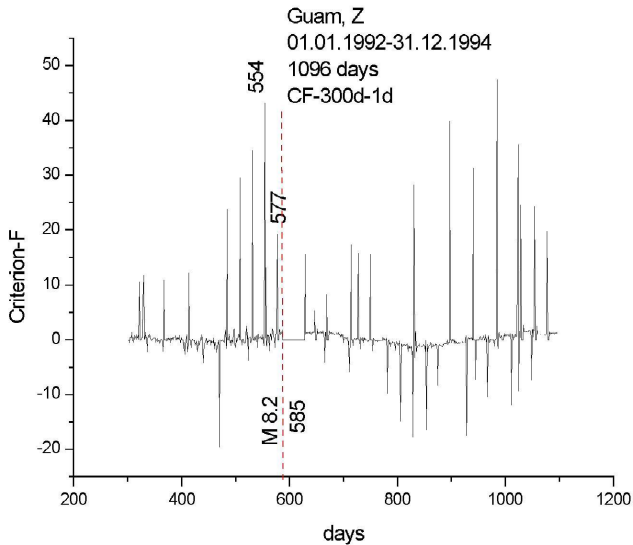
The results of calculation of the non-stationary factor $C_F(t_k)$ with using different values of T (value of the averaging window interval) and ΔT (value of the window shifts) for the Z component of ULF time series are presented. We know that Z components is much more sensitive to the crustal activity than the horizontal ones (Hayakawa et al., 1996), so that we have paid particular attention to this Z component. Note that Eq. (1) can be used to find a factor of non-stationarity in the cases when there are gaps in the set of analyzing data. In these cases, the sets of time intervals under calculation of the $\Phi^{(2)}(\tau)$ function for every delay parameter τ can be different. If one or both ends of the intervals fall within the gap, the contribution of the interval under the calculation of $\Phi^{(2)}(\tau)$ is equal zero, and we call such intervals the “empty intervals”. It means that the statistics could be different for calculation of the mean values, which are the $\Phi^{(2)}(\tau)$ functions for different τ . To be specific, we will choose a maximal part $b(\%)$ of the empty intervals as a parameter. If the percentage of the empty intervals exceeds b , we will omit calculating the factor of non-stationarity, and substitute $C(t_{k+1})=0$. In other words, we have “empty intervals” for the $C(t_{k+1})$ dependence. We will choose below $b=20\%$.

We use the “high-frequency” components of the signals, because the criterion factors $C_F(t_k)$ demonstrated clearer results as compared to $C_G(t_k)$. The problem is to reveal the FNS non-stationary factors and to understand whether these factors could be considered as precursors of the earthquake, which appeared in this region during the observed time. There was the largest event during the 1992–1994 years at the Guam region at $t^*_c=585d$, which corresponded to the event on 8 August 1993 ($M=8.2$) as indicated by No. 10 earthquake in Table 1. As already shown in Table 1, there have been no earthquake before this extremely large earthquake, though there have been taking place some earthquakes in the area away from the ULF observatory as seen in Table 1. The main idea here is to understand whether the T -value variations can help in distinguishing significant precursors to the earthquake.

The initial second data were used to get the initial minute data; every 60th second data were taken. Then we formed the hourly data (every 60th reading of the minute time series) as well as the daily time series (formed by every 24th reading of the hour time series). At first, we began to analyze the daily data. It is well known that large earthquakes are prepared during several years. That is why we began our analysis by considering large T-intervals for finding a precursor for the

Table 2. Peak values for several peaks before the Guam earthquake.

t_i^* , days	T=100 days	T=200 days	T=300 days	T=400 days	T=500 days	T=550 days
484	28.9	24.4	23.7	22.6		
508	24.9	29.5	29.5	29.6	31.3	
531	21.9	33.1	34.6	35.5	37.9	
554	22.0	37.1	43.1	47.4	51.1	53.0
577	8.5	15.1	19.1	21.6	23.0	24.3

**Fig. 2.** The temporal evolution of C_F factor during the whole period (3 years) of observation.

The vertical dotted line indicates the Guam earthquake occurred at the date of 585d with magnitude of 8.2. $T=300$ days and $\Delta T=1$ day.

case of $M=8.2$. In this case we processed the daily time series and calculated the $C_F(t_k)$ factors by choosing $T=550, 500, 400, 300, 200$ and 100 days as well as $\Delta T=1$ day for all cases. The results are calculated for $T=550$ (500,400, 300, 200, and 100) days, and $\Delta T=1$ day, but we present only one example among them in Fig. 1 with $T=300$ days and $\Delta T=1$ day. Many large peaks are found to be present in the calculated dependences as in Fig. 2. The appearance of every peak at different meanings of the current time means that the state of the geophysical medium is changed at these times. If anyone considers an ordinary time series (for the Z or other components) the appearance of any peak means that the measured value drops after rising. That is all. But in the case of the FNS non-stationary criteria the appearance of every peak means that the state of the medium is different before and after the peak. It means that the seismo-active medium could be reconstructed (changes its state) several times before the earthquake. It is interesting to study the dynamics

of the realized peaks during the whole time (3 years in our case). At first, several large peaks which appear after the main events, $t > t_c^*$, are not connected with large events (see the earthquake catalog in Table 1). At the same time the relative large non-stationarity factors before relative small ($M \sim 5.5-5.8$) earthquakes may indicate that the medium was reconstructed (rearrangements happened) strongly. It means the medium has become more volatile after the very large earthquake $M=8.2$. We can notice five significant peaks in C_F in Fig. 2 before the large earthquake at 585 day (Guam earthquake), which will be our greatest concern below.

We consider the averaging interval T as an “active” parameter, which helps us to extract some additional information. Let us consider the dynamics (the value changes) of the 5 peaks at t_i^* before the largest event $t < t_c^*$ by monitoring the value in C_F with changing the value of T . As seen from Fig. 2, we understand that 4 peaks occurred on 484, 508, 531 and 554 d are more enhanced than the 5th one on the day of 577th. The T interval was changed from 550, 500, 400, 300, 200 and 100 days, and the corresponding values of peaks in C_F are summarized in Table 2. It is seen from the table that these peaks become increased in their values when the T value is increased. Their values are found to become more enhanced in values, as compared with those at $t > t_c^*$ for large T (though the figures are not shown). This fact gives a strong ground to suppose that these peaks could be regarded as precursors to the large event ($M=8.2$) at $t_c^*=585$ d. Indeed, when the earthquake magnitude is larger, we expect more time interval for the event to be prepared and correspondingly for the seismo-active medium to rearrange its structure. It is possible to think that the 5 peaks many reflect the 5 stages of the complex processes of the medium rearrangement before the coming catastrophic earthquake. These precursors appeared at 101, 78, 54, 31 and 8 days before the event. It means that an appearance of a large value of the non-stationarity factor as a result of the FNS processing of observed data does not mean that the earthquake will come soon.

It follows from the previous figures (Fig. 2 as an example) that the C_F dependences for the averaging interval T more than 100 days cannot be used for looking for precursors for smaller events. Such precursors could be found if we use $T < 100$ days. Then we analyzed the hourly time

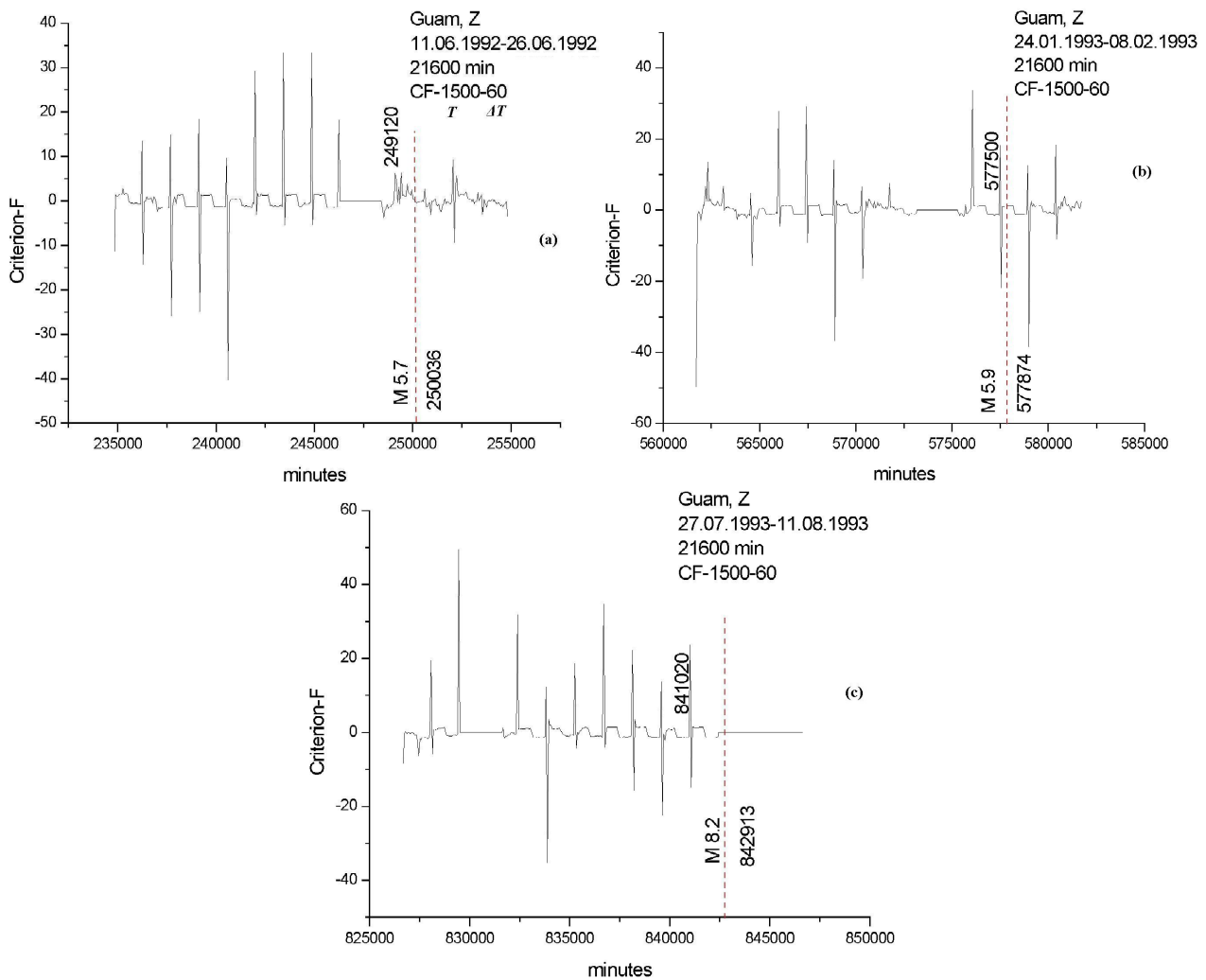


Fig. 3. The temporal evolution of C_F factor with $T=21\,600$ min ($=3600$ h= 150 days) and $\Delta T=60$ min ($=1$ h) for three different time intervals. (a) 11 June 1992 to 26 June 1992, (b) 24 January 1993 to 8 February 1993 and (c) 27 July 1993 to 11 August 1993.

series. At first, we compared the CF criterion for $T=100$ and 200 days, which were obtained by using the daily and corresponding hour time series: 100 days = 2400 h, and 200 days = 4800 h. We chose $\Delta T=24$ h= 1 day and 6 h= 0.25 day. Then some other cases with $T=50$ days, $\Delta T=6$ h and $T=25$ days, $\Delta T=6$ h were considered. However, this analysis (though not shown) gave the similar results (as for daily analysis) for the main event precursors. We could observe several new peaks, which could be considered as precursors to smaller events. At the same time it is necessary to fulfill a special analysis for every event, including analysis of the minute data to say about it. It is possible to do, but we would like to discuss the problem in general sense at first. In these cases we must choose smaller time series fragments in the interval around the considered event.

We illustrate the corresponding results by considering 3 time intervals for $T=21\,600$ min ($=3600$ h= 150 days): a) 11 June 1992–26 June 1992 (Fig. 3a); b) 24 January 1993–8 February 1993 (Fig. 3b); c) 27 July 1993–11 August 1993 (around $M=8.2$; Fig. 3c). There were relatively a large earthquake in Fig. 3a ($M=5.7$ on 22 June 1992 (No. 3 in Table 1)) and in Fig. 3b ($M=5.9$ on 5 February 1993 (No. 7 in Table 1)). Unfortunately, there were many gaps in any case, especially in Fig. 3c. Figures 3a–c demonstrate that the ULF signals can be used effectively for finding short-term precursors of earthquakes. Of course, these results must be tested by analyzing some other data, which do not contain any gaps. Furthermore, these two earthquakes (Nos. 3 and 7) are located about 300 km away from the ULF observatory, so that we wonder whether this FNS analysis would be able to detect far-distance earthquakes because Hayakawa and Hattori

(2004) have concluded that the sensitive area for seismogenic emissions is about 100 km from the observatory.

Note that the obtained results are not changed drastically if we choose $b=80\%$. The positions of the most parts of the non-stationary peaks remain the same. However, we find that a small part of the peaks disappear: the “empty intervals” for the $C(t_{k+1})$ dependence increase. In the case of the daily data, the differences between $b=50$ and 80% are substantial for the $T=100$ and 200 d in the intervals $t_{k+1}\sim 600\text{--}800$ days. However, for the $T\sim 300$ d and more, these differences are small. If we choose $b = 95\%$, these “empty intervals” spread significantly. It means there is some optimal meaning of the b parameter for every set of experimental data with gaps. We believe that the optimal value b is between 50 and 80% in our case.

6 Conclusion

We have presented a new method of FNS for the analysis of nonlinear process in any field. This method has been applied to the ULF data during the Guam earthquake on 8 August 1993, and we have been successful in finding out the detailed temporal evolution of the nonlinear process taking place in the lithosphere before the earthquake. That is, there must have taken place significant changes in the Earth’s crust 101, 78, 54, 31 and 8 days before the Guam earthquake. The lithosphere must have exhibited the step-like discontinuous changes in the focal zone. We do hope that this new method would be of great help in studying nonlinear process including the seismogenic ULF emissions.

Acknowledgements. One of the authors (M. Hayakawa) is grateful to Japan Society of Promotion of Sciences (#154031012), The Mitsubishi Foundation and NiCT (R and D promotion scheme funding international joint research) for their support. This work was also supported by Russian Fund of Fundamental Research (grant 05-02-17079), to which S. F. Timashev is grateful.

Edited by: J. Kurths

Reviewed by: two referees

References

- Bak, P., Tang, C., and Wiesenfeld, K.: Self-organized criticality: An explanation of $1/f$ noise, *Phys. Rev. Lett.*, 59, 381–384, 1987.
- Bak, P.: How Nature works (The Science of Self-organized Criticality), Oxford University Press, 201 pp., 1997.
- Burlaga, L. F. and Klein, L. W.: Fractal structure of the interplanetary magnetic field, *J. Geophys. Res.*, 91, 347–350, 1986.
- Erokin, N. S. and Moiseev, S. S.: General characteristics and development mechanisms of natural critical processes, *Geophysical Problem in the 21st Century* (in Russian), edited by: Nikolaev, A., Nauka, 160–182, 2003.
- Fraser-Smith, A. C., Bernardi, A., McGill, P. R., Ladd, M. E., Helliwell, R. A., and Villard Jr., O. G.: Low-frequency magnetic

field measurements near the epicenter of the Ms 7.1 Loma Prieta earthquake, *Geophys. Res. Lett.*, 17, 1465–1468, 1990.

- Gotoh, K., Hayakawa, M., and Smirnova, N.: Fractal analysis of the ULF geomagnetic data obtained at Izu peninsula, Japan in relation to the near by earthquake swarm of June–August 2000, *Nat. Hazard Earth Syst. Sci.*, 3, 229–236, 2003.
- Gotoh, K., Smirnova, N., and Hayakawa, M.: Fractal analysis of seismogenic ULF emissions, Special Issue on “Seismo Electromagnetics and Related Phenomena”, edited by: Hayakawa, M., Molchanov, O. A., Biagi, P., and Vallianatos, F., *Phys. Chem. Earth, Parts A/B/C*, 29, 4–9, 419–424, 2004.
- Hayakawa, M. (Ed.): Atmospheric and Ionospheric Electromagnetic Phenomena Associated with Earthquakes, *Terra Sci. Pub. Comp.*, Tokyo, pp. 996, 1999.
- Hayakawa, M., Molchanov, O. A., and NASDA/UEC team: Summary report of NASDA’s earthquake remote sensing frontier project, in: Special Issue on Seismo Electromagnetic and Related Phenomena, edited by: Hayakawa, M., Mochanov, O. A., Biagi, P., and Vallianatos, F., *Phys. Chem. Earth*, 29, 4–9, 617–626, 2004.
- Hayakawa, M., Itoh, T., and Smirnova, N.: Fractal analysis of ULF geomagnetic data associated with the Guam earthquake on August 8, 1993, *Geophys. Res. Lett.*, 26, 2797–2800, 1999.
- Hayakawa, M., Itoh, T., Hattori, K., and Yumoto, K.: ULF electromagnetic precursors for an earthquake at Biak, Indonesia on February 17, 1996, *Geophys. Res. Lett.*, 27, 1531–1534, 2000.
- Hayakawa, M.: NASDA’s Earthquake Remote Sensing Frontier Research, Seismo- electromagnetic Phenomena in the Lithosphere, Atmosphere and Ionosphere, Final Report 228 p., Univ. of Electro-Communications, March, 2001.
- Hayakawa, M. and Fujinawa, Y.: Electromagnetic Phenomena Related to Earthquake Prediction, *Terra Sci. Pub. Comp.*, Tokyo, Japan, pp. 477, 1994.
- Hayakawa, K., Kawate, R., Mochanov, O. A., and Yumoto, K.: Results of ultra-low-frequency magnetic field measurements during the Guam earthquake of 8 August 1993, *Geophys. Res. Lett.*, 23, 241–244, 1996.
- Hayakawa, M. and Molchanov, O. A. (Eds.): Seismo Electromagnetics: Lithosphere – Atmosphere – Ionosphere Coupling, TERAPUB, Tokyo, pp. 477, 2002.
- Hayakawa, M. and Hattori, K.: Ultra-low-frequency electromagnetic emissions associated with earthquakes, *Inst. Electr. Engrs. Japan, Trans. Fundamentals and Materials*, 124, 12, 1101–1108, 2004.
- Higuchi, T.: Approach to an irregular time on the basis of fractal theory, *Physica D*, 31, 277–283, 1988.
- Ida, Y., Hayakawa, M., Adalev, A., and Gotoh, K.: Multifractal analysis for the ULF geomagnetic data during the 1993 Guam earthquake, *Nonlin. Processes Geophys.*, 12, 157–162, 2005, <http://www.nonlin-processes-geophys.net/12/157/2005/>.
- Kapiris, P. G., Balasis, G. T., Kopanas, J. A., Antonopoulos, G. N., Pertzakis, A. S., and Eftaxias, K. A.: Scaling similarities of multiple fracturing of solid materials, *Nonlin. Processes Geophys.*, 11, 137–151, 2004, <http://www.nonlin-processes-geophys.net/11/137/2004/>.
- Kopytenko, Y. A., Matishvili, T. G., Voronov, P. M., Kopytenko, E. A., and Molchanov, O. A.: Detection of ultra-low-frequency emissions connected with the Spitak earthquake and its after-shock activity, based on geomagnetic pulsations data at Dusheti

- and Vatzia observations, *Phys. Earth Planet. Inter.*, 77, 85–95, 1993.
- Molchanov, O. A., Kopytenko, Y. A., Voronov, P. M., Kopytenko, E. A., Matiashvili, T. G., Fraser-Smith, A. C., and Bernardi, A.: Results of ULF magnetic field measurements near the epicenters of the Spitak ($m_s=6.9$) and Loma Prieta ($M_s=7.1$) earthquakes: Comparative analysis, *Geophys. Res. Lett.*, 19, 1495–1498, 1992.
- Molchanov, O. A. and Hayakawa, M.: Generation of ULF electromagnetic emissions by microfracturing, *Geophys. Res. Lett.*, 22, 3091–3094, 1995.
- Vallianatos, F. and Tzanis, A.: A model for the generation of precursory electric and magnetic fields associated with the deformation rate of the earthquake focus, in: *Atmospheric and Ionospheric Electromagnetic Phenomena Associated with Earthquakes*, edited by: Hayakawa, M., TERRAPUB, Tokyo, 287–306, 1999.
- Smirnova, N., Hayakawa, M., Gotoh, K., and Volobuev, D.: Scaling characteristics of ULF geomagnetic field at the Guam seismoactive area and their dynamics in relation to the earthquake, *Nat. Hazards Earth Syst. Sci.*, 1, 119–126, 2001, <http://www.nat-hazards-earth-syst-sci.net/1/119/2001/>.
- Timashev, S. F.: Flicker-noise spectroscopy as a tool for analysis of fluctuations in physical system, *Noise in Physical Systems and 1/f Fluctuations*, World Scientific, edited by: Bosman, G., World Scientific, 775–778, 2001.
- Timashev, S. F. and Vstovsky, G. V.: Flicker noise spectroscopy in the analysis of chaotic time series of dynamic variables and the problem of the signal-to-noise ratio, *Elektrokhimiya* 39(2), 149–162, 2003.
- Turcott, D. L.: *Fractal and Chaos in Geology and Geophysics*, 2nd Edition, Cambridge Univ. Press, 1997.